

EXPERIMENTAL AND NUMERICAL PROGRESSIVE FAILURE ANALYSIS IN OPEN-HOLE TENSILE TESTS OF QUASI-ISOTROPIC COMPOSITE LAMINATES

Sina AhmadvashaAghbash¹, Fatih E. Öz¹, Mahoor Mehdikhani², Stepan V. Lomov² and Nuri Ersoy^{1,3}

¹Department of Mechanical Engineering, Boğaziçi University, Bebek, 34342, Istanbul, Turkey
Emails: sina.ahmadvashaghbash@boun.edu.tr, fatih.oz@boun.edu.tr

²Department of Materials Engineering, KU Leuven, Kasteelpark Arenberg 44, 3001 Leuven
Emails: mahoor.mehdikhani@mtm.kuleuven.be, stepan.lomov@kuleuven.be

³Department of Engineering, Design, and Mathematics, University of West England, BS16 1QY, Bristol, United Kingdom

Email: nuri.ersoy@boun.edu.tr, Web Page: <http://www.kompozit.boun.edu.tr>

Keywords: Open-Hole Tension, Progressive Failure Analysis, Cohesive Zone Model, Acoustic Emission, Digital Image Correlation

Abstract

A Finite Element Analysis (ABAQUS/Implicit) was performed to predict the progressive failure behavior (intralaminar failure and delamination) of Open-Hole Tension (OHT) specimens with $[+45_2/90_2/-45_2/0_2]_s$ layup. Initiation and evolution of delamination were modelled based on the Cohesive Zone Model. Numerical and experimental benchmarking studies were conducted to evaluate Mode I and Mode II fracture toughnesses. Damage modes and their sequence were experimentally identified with *in-situ* damage detection techniques. Acoustic Emission was used primarily to investigate the overall damage behavior. Digital Image Correlation and edge microscopy were utilized simultaneously to capture the damage on the surface and micro-cracks at the inner plies respectively. Damage initiates with micro transverse cracks at the 90° plies, followed by surface cracks in the +45° plies and delaminations at the $\pm 45^\circ/90^\circ$ interface causing a load drop in the stress-strain curve. Finally, delaminations propagated extensively at the $\pm 45^\circ/90^\circ$ interface with delaminations at the $-45^\circ/0^\circ$ interface causing major load drops through the end of the test. Finite element model successfully predicts the stress-strain response and sequence of the damage modes in OHT specimens with less than 10 % error.

1. Introduction

The damage mechanisms in composites are related to various failure modes under a variety of loading conditions. The failure modes in composite laminates can be divided into two classes: intralaminar matrix cracking and delaminations. The latter is considered as a catastrophic failure mode since it degrades the stiffness of the composite part considerably. The structural application of composites generally demands the existence of holes or predefined cracks. Investigation of an efficient finite element model that can cover both intralaminar and interlaminar failure modes in open-hole tension testing of composites is considered worthwhile.

Coelho et al. [1] constructed a simplified 3D model to predict damage initiation and progression of Open-Hole Tension (OHT) that only relies on the capabilities of ABAQUS (composite lay-up method and continuum shell elements). This model with a reasonable accuracy predicts the fiber and matrix crack extension and the load-drop. Since cohesive elements or surfaces are not applied between plies it

fails to capture the delamination phenomena. B.Y. Chen et al. [2] investigated the size effects on open-hole tensile composites. In their numerical study, it is observed that excluding delamination will give mesh-dependent and overvalued strengths which make delamination as an inevitable consideration in Progressive Failure Analysis (PFA). The variation of interface parameters required for interlaminar failure modelling including shear strength σ_{sc} ($=\sigma_{st}$) and mode II fracture energy G_{sc} are perceived to have a negligible effect on damage patterns and pull-out failure mode. However, the delamination is observed to be extremely sensitive to these two parameters which puts the experimental measurements of them on the spot.

Wisnom et al. [3] experimentally investigated the role of delamination in the intra-ply strength and failure mechanisms. The hole diameter is reported to have a direct effect on the quasi-isotropic laminate strength. By enlarging the notch diameter the strength converges to the strength of wide unnotched specimens. In other words, the delamination failure becomes more dominant as the hole diameter decreases. In ply-level scaled laminates the delamination extension is reported to be the ultimate failure mode, whereas in sub-laminate level scaled laminates, the ultimate failure mode is fiber breakage in 0° ply. Ridha et al. [4] applied Tsai-Wu criterion in conjunction with the maximum-stress criterion to simulate matrix and fiber failure initiation respectively. The delamination between plies is modelled using cohesive elements and a traction separation law in ABAQUS. As an alternative approach to the linear softening method for in-plane failure, zigzagging method (UMAT code) has been preferred as a stabilization algorithm to achieve converged results and also damage extension even after load drop. Higuchi et al. [5] constructed a predictive model using coupled extended finite element method and cohesive zone model (XFEM/CZM) based on quasi-isotropic 3D XFEM approach proposed by Nagashima et al. [6]. The elasto-plastic constitutive law is implemented to count for non-linear behavior before peak load. Matrix crack and delamination extension are modeled with combining XFEM and CZM where zigzagging softening law used in later to ease computational convergence. Furthermore, fiber failure is modeled using Weibull criterion [7]. This model is considered to successfully predict the strength of OHT specimens.

Based on the experimental works of Green et al. [8] in a numerical study Bao et al. [9] employed surface-based cohesive interaction rather than cohesive elements to model the delamination and splitting. The reason behind this approach lies in the fact that using cohesive surfaces provides the possibility to assign different mesh patterns for different plies. Using aligned mesh in fiber direction of each ply will allow the precise prediction of matrix crack paths. Erçin et al. [10] examined the size effects on OHT and Open-Hole Compression laminates experimentally and numerically. The Digital Image Correlation (DIC) method in conjunction with MATLAB scripts has been applied to detect the First-Ply Failure load and progressive damage mechanisms on the top 90° ply in $[90/45/0-45]_s$ laminates with varying hole diameter. It is concluded that all the OHT coupons form transverse matrix cracks on the top ply originating from the hole boundary and also from free edges [11, 12].

None of the above-mentioned papers did an extensive damage evolution observation, either using optical or Acoustic Emission techniques to correlate the results of progressive damage analysis with the observed damage progression. Although some studies observed the specimens optically for damage progression, these observations are limited to surface cracks. The main contribution of this study is to interpret how damage evolves using two optical techniques, namely DIC and edge microscopy, and Acoustic Emission (AE) technique to detect damage modes within the specimens in order to correlate the progressive damage model predictions with experimentally observed damage modes. Furthermore, experimentally measured material properties are used for setting up the model parameters in progressive failure analysis to obtain a better correlation. For damage initiation of in-plane failure, Hashin's failure criterion is suggested to be implemented into the model mainly due to its high accuracy that can be obtained with a low number of material properties. In conjunction with damage initiation, damage evolution law for in-plane failure needs to be defined in terms of fracture energy with linear softening. Initiation and evolution of delamination between adjacent plies are considered in the laminate for a realistic simulation.

2. Experimental Procedure

The material used is IM7/8552, a unidirectional (UD) carbon-fibre/epoxy pre-preg system, with a ply thickness of 0.184 mm. Quasi-isotropic laminates with a centrally located circular hole were tested under displacement control according to ASTM D5766 [13] test standard with AE sensors attached to the specimen to acquire Acoustic Emission signals. Tension test is conducted in KU Leuven with electro-mechanical Instron® 4505 test device. The wide surface of the specimen is observed by a camera and DIC technique using VIC 2D software has been applied for extensometry measurements. A second camera with a higher resolution is used to capture micro damage progression on the edges of the specimens. The k-means++ clustering algorithm is applied to cluster similar AE events [14, 15].

3. Overview of the Cohesive Zone Model (CZM)

The primary study on CZM backs to the works of Barenblatt [16] and Dugdale [17] on the fracture behaviour around the crack tip in brittle materials and steel. Hillerborg et al. [18] combined fracture mechanics with Finite Element Analysis (FEA) to obtain more realistic results on crack formation and evolution. The CZM considers a cohesive zone (process zone) ahead of the crack tip to count for crack initiation and propagation by using sets of constitutive equations such as traction-separation laws. The traction-separation laws associate the opposing tractions of the cohesive zone to the opening displacements. Depending on the crack mode (Mode I, II or III), the traction-separation laws are defined based on initial stiffness, maximum traction, interfacial strength and the area under the stress-displacement curve which is considered as the critical energy release rate G_c [19]. A linear elastic-linear softening behaviour is generally selected to be implemented in the simulations [20]. Based on the CZM approach, interface cohesive elements can be assigned in FEA to simulate delamination.

4. Determination of Interlaminar Fracture Toughness

Double Cantilever Beam (DCB) and End Notched Flexure (ENF) tests are performed according to ASTM D5528 [21] and ASTM D7905 [22] test standards for evaluation of Mode I and Mode II fracture toughnesses respectively. In FEA, in order to increase the element length, which would directly reduce the run time, a parametric study is carried out. The CZM parameters such as characteristic length, interfacial strength and stiffness are optimized to attain a good correlation between test data and model predictions for DCB and ENF tests. According to works of Turon et al. [23], cohesive zone length can be artificially increased by reducing the interfacial strength while keeping the fracture toughnesses constant. With this approach, the DCB and ENF test load-displacement results are compared with their 3D FE model in Fig. 1.

5. Finite Element Model

For numerical analysis of progressive failure in OHT composite laminates, capabilities of the ABAQUS/Standard finite element software package is explored. The OHT specimen configuration used in this study is prepared according to the ASTM D5766 [13] test standard and is demonstrated in Fig. 2. Note that the gripping region is not considered in the proposed model. A 3D deformable solid extruded part is created with a thickness of 1.479 mm including 0.184 mm thick composite plies and 0.001 mm thick cohesive layers. The sketched part is then partitioned into 8 composite plies with 7 cohesive plies in between. To improve convergence, accuracy and efficiency in composite material simulations Autodesk® Helius PFA plug-in for ABAQUS has been used to create composite and cohesive materials using properties as given in Table 1 and Table 2, respectively. Composite plies are defined to the partitions by assigning composite layup with continuum shell element type option while cohesive properties have been applied to the partitioned cohesive layers using traction separation response.

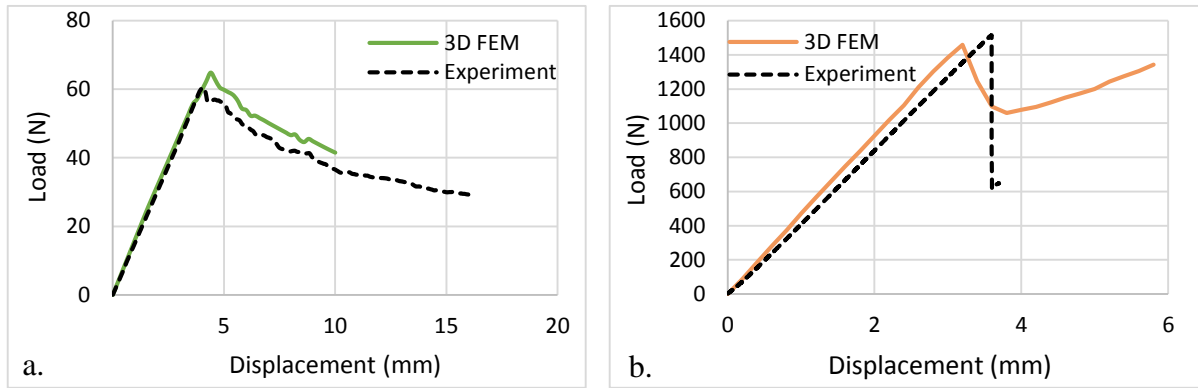


Figure 1. Load-displacement responses of 3D FE models and experimental tests, a. DCB test, b. ENF test

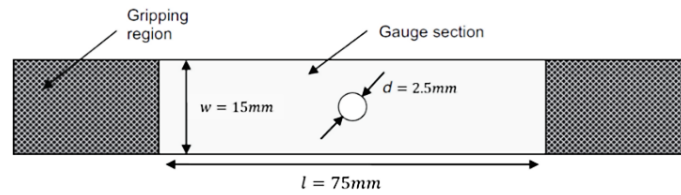


Figure 2. Specimen configuration

Table 1. Material Parameters for UD Composite [24]

E_1 (GPa)	E_2 (GPa)	G_{12} (GPa)	G_{23} (GPa)	ν_{12}	ν_{23}	σ_1^T (MPa)	σ_1^C (MPa)	σ_2^T (MPa)	σ_2^C (MPa)	τ_{12}^S (MPa)
142.84	10	5.571	3.278	0.263	0.525	2105	1531	51	26	114.5

Table 2. Interlaminar strength, fracture energy and stiffness parameters for cohesive elements

σ_{33c} (MPa)	σ_{13c} (MPa)	G_{Ic} (KJ/m ²)	G_{IIc} (KJ/m ²)	K_{nn} (N/mm ³)	K_{ss} (N/mm ³)
81	114	0.28	2.59	2.72E+006	2.72E+006

An implicit step is generated for the analysis. The general solution controls editor for the step allows the modification of the convergence algorithms and accuracy of time integration. The time incrementation control parameters have been increased from their default values.

The whole part is meshed with hexahedral elements using swept meshing technique. The Medial Axis Algorithm is preferred to minimize the mesh transition and distortion. Due to the distinctive directional behaviour of continuum shell and cohesive elements, a through the thickness mesh stack direction must be assigned to the part in the mesh module. Continuum shell elements (SC8R) with linear geometric order and enhanced hourglass control and cohesive elements (COH3D8) are selected as element types for modeling composite plies and cohesive layers respectively. The element deletion option is activated in assigning the element types. A nodal displacement with a tabular amplitude is applied to the tip node, which is connected to all the nodes on the right edge surface of the specimen with using an equation type constraint. Assigned boundary conditions are represented in Fig. 3.

Fig. 4 shows the consistency between the tensile stress-strain response and its FE predictions. Damage progression at different strain levels was compared with FE predictions in Fig. 5. Damage was observed to initiate with micro transverse cracks at 90° plies, followed by surface cracks in the +45° plies. Then delaminations occurred at the ±45°/90° interface that caused load drop in the stress-strain curve. Finally, delaminations propagated extensively at this interface with delaminations at the -45°/0° interface which caused higher load drops through the end of the test.

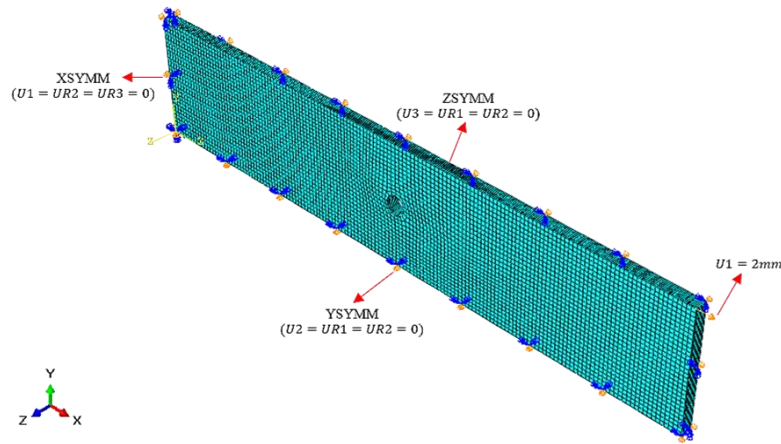


Figure 3. Boundary conditions used for the OHT analysis

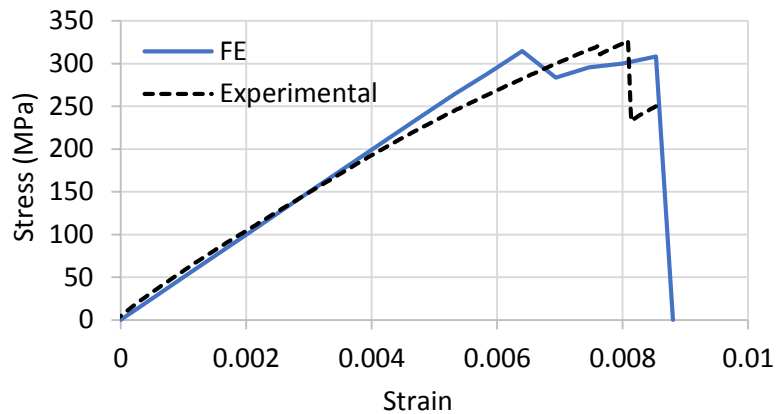


Figure 4. Comparison of stress-strain curves

Summary of cluster groups and accumulation of AE clusters throughout a test for $[+45_2/90_2/-45_2/0_2]_s$ laminate is presented in Fig. 6. A detailed correlation is done between the accumulation of AE events and optical damage detection techniques in [14]. It is seen that delamination propagation in the ε_2 DIC strain map is consistent with the accumulation of CL3 events. These events are first localized around the hole region, then propagate to further regions of the specimen after 7000 μs . So CL3 events represent macro delaminations at the ±45°/90° and the -45°/0° interfaces. Accumulation of CL4 events are highly consistent with the propagation of transverse cracks at the 90° and the -45° plies. It is observed that cracks at surface +45° plies are registered with high amplitude CL1 events. Registration of CL1 and CL4 events are seen to stop after the load drops in the stress-strain curves. Because, load drops occur due to delaminations and cause the propagation macro delaminations and this stops the propagation of transverse cracks and surface cracks. Only delamination propagates after the load drops and stops the registration of CL1 and CL4 events. Finally, low amplitude/low frequency events represent micro delaminations at ±45°/90° interfaces.

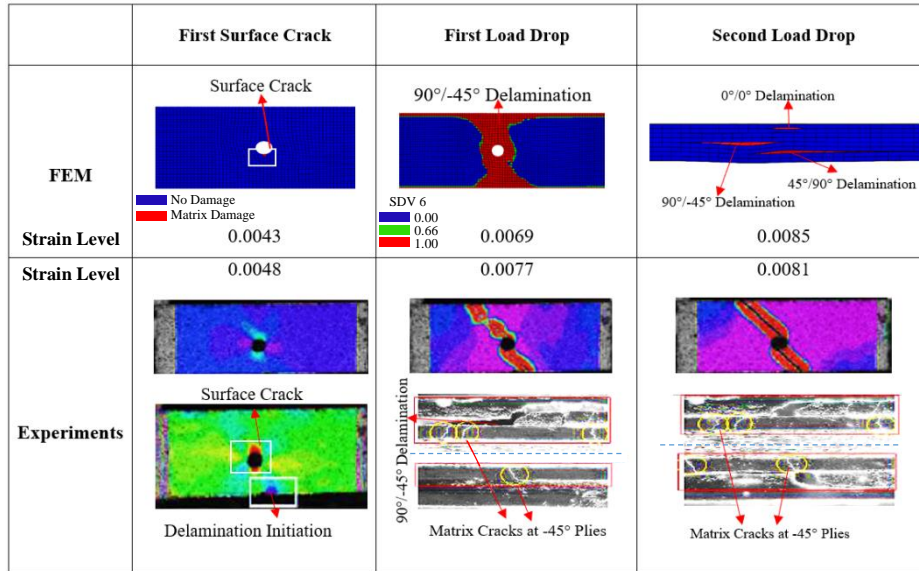


Figure 5. Comparison of the damage modes progression

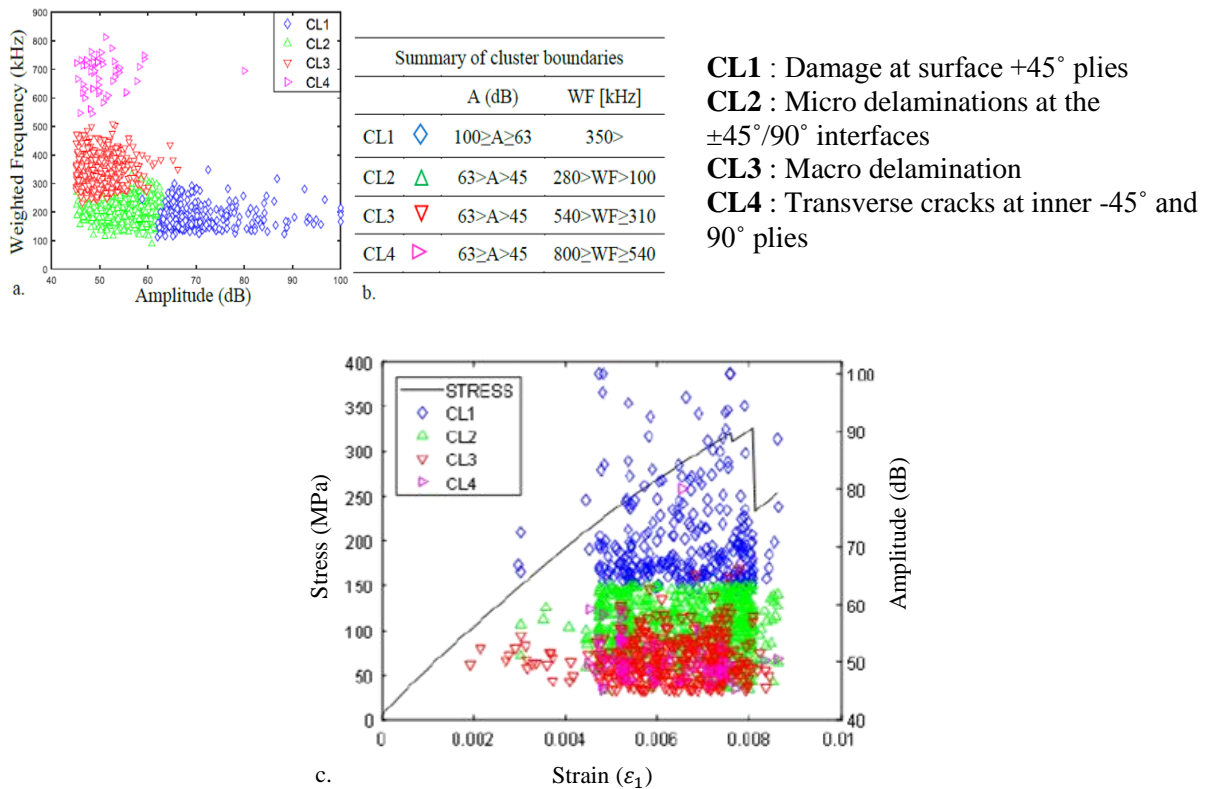


Figure 6. Cluster groups, a. Clusters from a representative test, b. Cluster boundaries, c. Accumulation of clusters during the test [14, 15]

6. Conclusions

In this study, the progressive failure behavior of the OHT specimens was analyzed both numerically and experimentally. The progressive damage during tensile loading is simulated numerically by taking into

account both intralaminar failure and delamination. Initiation and evolution of delamination are based on the CZM. Numerical and experimental benchmarking studies have also been conducted to evaluate mode I and mode II interlaminar fracture toughness by performing DCB and ENF tests. In experimental part, damage progression in OHT with a 2.5 mm central hole was investigated with AE technique. Optical instruments have been used to obtain reliable correlations with damage modes and the AE events. DIC and in-situ edge observation are applied simultaneously during the tensile tests of quasi-isotropic laminates. High-frequency events are registered due to the existence of transverse cracks at inner $\pm 45^\circ$ plies or 90° plies, whereas high amplitude events around the hole are due to delaminations in the $\pm 45^\circ/90^\circ$ plies. This model can successfully predict the damage progression and ultimate strength of the OHT specimens.

Acknowledgments

Authors acknowledge the support of the Boğaziçi University Research Fund, Istanbul Development Agency (ISTKA) and TUBITAK BİDEB 2214-A under project codes 10020/15A06D3, ISTKA/BIL/2012/58 and 1059B141600673 respectively. S.V. Lomov holds the Toray Chair on Composites at KU Leuven, the support of which is gratefully acknowledged.

References

- [1] A.M.G. Coelho, J.T. Mottram and K.A. Harries. Finite element guidelines for simulation of fibre-tension dominated failures in composite materials validated by case studies. *Composite Structures*, 126:299–313, 2015.
- [2] B.Y. Chen, T.E. Tay, P.M. Baiz, and S.T. Pinho. Numerical analysis of size effects on open-hole tensile composite laminates. *Composites Part A: Applied Science and Manufacturing*, 47:52–62, 2013.
- [3] M.R. Wisnom and S.R. Hallett. The role of delamination in strength, failure mechanism and hole size effect in open hole tensile tests on quasi-isotropic laminates. *Composites Part A: Applied Science and Manufacturing*, 40:335–342, 2009.
- [4] M. Ridha, C.H. Wang, B.Y. Chen and T.E. Tay. “Modelling complex progressive failure in notched composite laminates with varying sizes and stacking sequences. *Composites Part A: Applied Science and Manufacturing*, 58:16–23, 2014.
- [5] R. Higuchi, T. Okabe and T. Nagashima. Numerical simulation of progressive damage and failure in composite laminates using XFEM/CZM coupled approach. *Composites Part A: Applied Science and Manufacturing*, 95:197–207, 2017.
- [6] T. Nagashima and M. Sawada. Development of a damage propagation analysis system based on level set XFEM using the cohesive zone model. *Computers and Structures*, 174:42–53, 2016.
- [7] S.R. Hallett, B.G. Green, W.G. Jiang and M.R. Wisnom. An experimental and numerical investigation into the damage mechanisms in notched composites. *Composites Part A: Applied Science and Manufacturing*, 40:613–624, 2009.
- [8] B.G. Green, M.R. Wisnom and S. R. Hallett. An experimental investigation into the tensile strength scaling of notched composites. *Composites Part A: Applied Science and Manufacturing*, 38:867–878, 2007.
- [9] H. Bao and G. Liu. Progressive failure analysis on scaled open-hole tensile composite laminates. *Composite Structures*, 150:173–180, 2016.
- [10] G.H. Erçin, P.P. Camanho, J. Xavier, G. Catalanotti, S. Mahdi and P. Linde. Size effects on the

- tensile and compressive failure of notched composite laminates. *Composite Structures*, 96:736–744, 2013.
- [11] K. Hoos, E.V. Iarve, M. Braginsky, E. Zhou and D.H. Mollenhauer. Static strength prediction in laminated composites by using discrete damage modeling. *Journal of Composite Materials*, 51:1473-1492, 2017.
- [12] M.J. Swindeman, E.V. Iarve and R.A. Brockman. Strength prediction in open hole composite laminates by using discrete damage modeling. *AIAA Journal*, 51:936-945, 2013
- [13] ASTM D5766/D5766M-11. Standard test method for open-hole tensile strength of polymer matrix composite. *American Society for Testing and Materials*, 2013.
- [14] F.E. Öz, N. Ersoy, M. Mhedikhani and S.V. Lomov. In-Situ investigation of damage mode progression in open-hole quasi-isotropic laminates. *Proceedings of the 18th European Conference on Composite Materials ECCM-18*, Athens, Greece, 2018.
- [15] F.E. Öz, N. Ersoy and S.V. Lomov. Do high-frequency acoustic emission events always represent fibre failure in CFRP laminates? *Composites Part A: Applied Science and Manufacturing*, 103:230–235, 2017.
- [16] G. I. Barenblatt. The mathematical theory of equilibrium cracks in brittle fracture. *Advances in Applied Mechanics*, 7:55–129, 1962.
- [17] D.S. Dugdale. Yielding of steel sheets containing slits. *Journal of the Mechanics and Physics of Solids*, 8:100–104, 1960.
- [18] A. Hillerborg, M. Modeer and P.E. Petersson. Analysis of crack formation and crack growth in concrete by means of fracture mechanics and finite elements. *Cement and Concrete Research*, 6:773–782, 1976.
- [19] K. Song, C. Davila and C. Rose. Guidelines and parameter selection for the simulation of progressive delamination. *ABAQUS User's Conference*, 1–15, 2008.
- [20] P.P. Camanho, C.G. Dávila and M.F. de Moura. Numerical simulation of mixed-mode progressive delamination in composite materials. *Journal of Composite Materials*, 37:1415–1424, 2003.
- [21] ASTM D5528-13. Standard test method for Mode I interlaminar fracture toughness of unidirectional fiber-reinforced polymer matrix composites. *American Society for Testing and Materials*, 2013.
- [22] ASTM D7905/D7905M-14. Standard test method for Mode II interlaminar fracture toughness of unidirectional fiber-reinforced polymer matrix composites. *American Society for Testing and Materials*, 2014.
- [23] A. Turon, C.G. Dávila, P.P. Camanho and J. Costa. An engineering solution for mesh size effects in the simulation of delamination using cohesive zone models,” *Engineering Fracture Mechanics*, 74:1665–1682, 2007.
- [24] F.E. Öz. Micromechanical progressive damage model for predicting resin dominated strength values of fibre reinforced composites under various types of loading. *M.Sc. Thesis*, Boğaziçi University, 2012.